Proc. Lunar Sci. Conf. 8th (1977), p. 841–863.
Printed in the United States of America

12054 and 76215: New measurements of interplanetary dust and solar flare fluxes

D. A. MORRISON

NASA Johnson Space Center, Houston, Texas 77058

E. ZINNER

McDonnell Center for Space Sciences, Washington University, St. Louis, Missouri 63130

Abstract—Studies of lunar samples 12054 and 76215 have provided results pertinent to questions of the mass distribution and flux of micrometeoroids, the calibration of the solor-flare track production rate, possible variations in solar activity, the magnitude of solar-wind erosion, and whether or not the interplanetary dust flux has varied with time.

The microcrater size frequency distribution of 12054 shows that micrometeorites have a bimodal mass distribution. The ratio of 0.1–500 μ diameter craters is about 1×10^8 for both 76215 and 12054. This ratio and the microcrater distribution indicate more efficient production of beta-micrometeoroids by approximately an order of magnitude than the distributions of other workers.

The solar cosmic-ray track age for 12054 is $1.75 \pm 0.25 \times 10^5$ yr, and the ^{26}Al exposure age is $1.60 \pm 0.5 \times 10^5$ yr. The track age for 76215 is 16,000 yr and the abundances of solar-wind implanted Mg and Fe indicates exposure ages of 2.1 and 2.4×10^4 yr respectively. The agreement between exposure ages measured in different ways confirms the Blanford track production model, and no variation in solar activity is indicated over a 2×10^6 yr period.

Submicron-sized features present on the surface of 76215,77 throughout its lunar surface exposure place an upper limit of 0.03 Å/yr on solar wind erosion.

The micrometeoroid fluxes derived from 76215 and 12014 are the same, and in agreement with interplanetary dust fluxes at 1 a.u. measured by Heos II and Pioneer 8/9. No variation for 5×10^5 yr in the interplanetary dust flux is indicated.

INTRODUCTION

THE RETURN OF LUNAR SAMPLES by the Apollo missions offered, among many others, a unique opportunity to study solar activity and interplanetary dust. From the special perspective of the work reported here we consider lunar rock samples which were exposed on the lunar surface as solar flare particle and micrometeoroid detectors. Heavy solar flare particles produce nuclear tracks in lunar crystals, micrometeoroid impacts produce microcraters on crystalline and glass surfaces.

The studies of microcraters in lunar materials extend modern optical and satellite observations into the past. Furthermore, direct present-day measurements are limited by statistics because of the low flux of interplanetary dust particles. Lunar sample detectors have exposure times which are many orders of magnitude larger than those of satellite detectors. Thus, lunar sample measurements can in principle provide us with important information on the origin of the interplanetary dust, on mechanisms responsible for its size distribution and on variations of the dust flux in the past.

Early crater measurements on lunar rocks (e.g., Hörz *et al.*, 1975) yielded a wealth of data but, for certain objectives, also suffered from the lack of suitable samples. Crater size distributions obtained by different experimenters, who did not all pay sufficient attention to problems of erosion, shielding, shadowing, and the accumulation of secondary accretionary debris, which all can crucially affect crater size measurements, differed considerably. It was not until recently that sufficiently uneroded surfaces suitable for crater counts were found to establish a crater size distribution in the diameter range from 0.1 to 500 μ (Morrison and Zinner, 1976). But even then this crater size distribution was still based on measurements of craters on various different samples which subsequently were normalized with respect to one another and combined into a single curve. It furthermore did not agree with the distribution obtained by other investigators (Fechtig *et al.*, 1975) which was also assembled from data on many rocks. A definitive measurement of the whole crater size range from a single surface was still outstanding.

There is a similar disagreement on the subject of solar flare tracks. Early measurements in lunar rocks (e.g., Crozaz *et al.*, 1971; Yuhas *et al.*, 1972) failed to verify the steep falloff of the track density as a function of depth that was expected from satellite measurements as well as from the track analysis of the Surveyor glass (Crozaz and Walker, 1971; Fleischer *et al.*, 1971; Price *et al.*, 1971). It was realized that the erosion of rock surfaces by micrometeoroid impacts was responsible for this flattening of the gradient of the track density versus depth distribution. On rock 68815 where only the top millimeter was affected by erosion, Walker and Yuhas (1973) could derive an empirical track production spectrum of galactic cosmic rays. This spectrum could be used for the measurement of "galactic cosmic ray exposure ages." For depths less than 1 mm where solar flare contributions dominate the track production, the data from the Surveyor glass which had sampled only a period of 2.6 yr provided the then best available "standard" solar flare Fe track production spectrum.

This situation improved considerably when Hutcheon *et al.* (1974), Yuhas (1974), and Blanford *et al.* (1975) found rock samples which were uneroded enough to allow the determination of a long range average track production rate from lunar rock crystals themselves. Hutcheon *et al.* (1974) and Yuhas (1974) accomplished this by relating the solar flare track densities to galactic cosmic ray track densities at larger depth and thus to the Walker and Yuhas (1973) galactic track production. The production spectrum of Blanford *et al.* (1975) is based on rock 64455 with a known Kr–Kr galactic exposure age. These track production rates could then be used to determine the "solar flare exposure age" of rock samples for which steep solar flare gradients could be measured (Hutcheon, 1975; Morrison and Zinner, 1975, 1976).

Unfortunately, there is still a sizeable disagreement between these three "standard" track production spectra (see Zinner and Morrison, 1976) which implies a correspondingly large uncertainty in the inferred solar flare exposure ages. Although the slopes of most track density gradients in lunar rock samples agree better with the slopes of the Blanford *et al.* (1975) and Yuhas (1974)

spectra and although the fact that only the Blanford *et al.* (1975) spectrum is based on an independent Kr–Kr age favors this measurement, it is important to obtain additional data to help eliminate the present-day uncertainties.

The measurement of both microcraters and solar flare tracks on the same samples has been used by Hutcheon (1975) and Morrison and Zinner (1975) to compare the micrometeorite flux in directions in and out of the ecliptic. Furthermore, it has been used to compare the relative fluxes of solar flare and micrometeorite particles over different periods in the past. Whereas others arrived at a change in the dust flux (Hartung and Storzer, 1975) or the solar flare activity (Zook *et al.*, 1976) in the past from such measurements our previous data do not imply any relative changes. Under the assumption of constancy of either quantity we could derive a crater production rate (Morrison and Zinner, 1976). This production rate in turn can be used to date the surface residence of lunar samples ("crater exposure age") in cases where other methods are not applicable.

In this paper we present new microcrater and solar flare particle track data from a study of samples of lunar rocks 12054 and 76215. The work on 12054 is part of a consortium effort organized by J. B. Hartung. These data provide a new standard for the microcrater size distribution and crater production, contribute importantly to our understanding of the constancy of the solar flare particle and micrometeoroid flux in time, and finally help to narrow the existing uncertainty in the solar flare track production rate.

12054 is a superior sample for crater and track studies because it has a thin uneroded glass surface (on which microcraters are easily recognizable) superimposed on a crystalline substrate which serves as an efficient detector of cosmic ray particle tracks. The exposure history of the rock is a simple one-stage sequence in terms of exposure to micrometeorites and the numbers of microcraters from less than 0.1 μ to several hundred microns diameter are great enough to produce satisfactory counting statistics over the entire diameter range. Consequently it is possible to construct a size frequence distribution which for the first time is derived from measurements on a single rock surface. Because the substrate is crystalline, cosmic ray track analysis is not complicated by the large corrections required for tracks in glasses (Hartung and Storzer, (1974).

Our work on 76215 extends previous results Morrison and Zinner, 1975, 1976). In this case the microcrater record and the solar flare particle track record were studied on the same anorthite crystal. These measurements can then be compared with the analysis of solar wind species on the same surface reported by Zinner *et al.* (This volume).

Sample Description and Experimental Methods

12054 is a 687 g glass coated rock (LSPET, 1970). Its lunar surface position at the time of collection was well documented and reproduced in the laboratory (Zook, 1976, pers. comm.). Microcraters were observed in the scanning electron microscope. All crater measurements were made on photo-mosaics of various magnifications. Magnifications were checked with a diffraction grating. Crater diameters are measured from rim to rim of the central pit. The samples were cut

normal to the surface and polished for track work. Cosmic ray particle tracks in plagioclase were etched for various times in 6.25 N NaOH held at 95°C. Track densities were measured on SEM photo-mosaics. The track production standard and parameters of Blanford *et al.* (1975) were used in exposure age calculations.

Counting errors in both cases were calculated as the number counted plus or minus its square root and divided by the area considered.

All of the samples were cleaned ultrasonically in Freon and gold coated before examination.

MICROCRATER RESULTS

Microcraters were counted on three samples of 12054 whose locations are shown in Fig. 1 together with the lunar surface orientation of the parent rock. Accumulative microcrater density distributions for 12054,54 and 12054,3 are shown in Fig. 2 and the distribution for 12054,55 shown in Fig. 3. The magnifications shown on the figures were selected to be most suitable for measuring craters within a diameter interval. The data are *not* normalized from one magnification set to the other nor otherwise corrected, including no correction for exposure geometry.

Also shown in Fig. 2 are crater densities determined optically by Hörz (1976, pers. comm.). These measurements were made on the side of the rock from which our samples were taken but included a much larger area. As in the case of the SEM measurements, no corrections have been made.

The surfaces of all three samples are overprinted by accretionary particles, principally various forms of glass. These have been considered in detail by

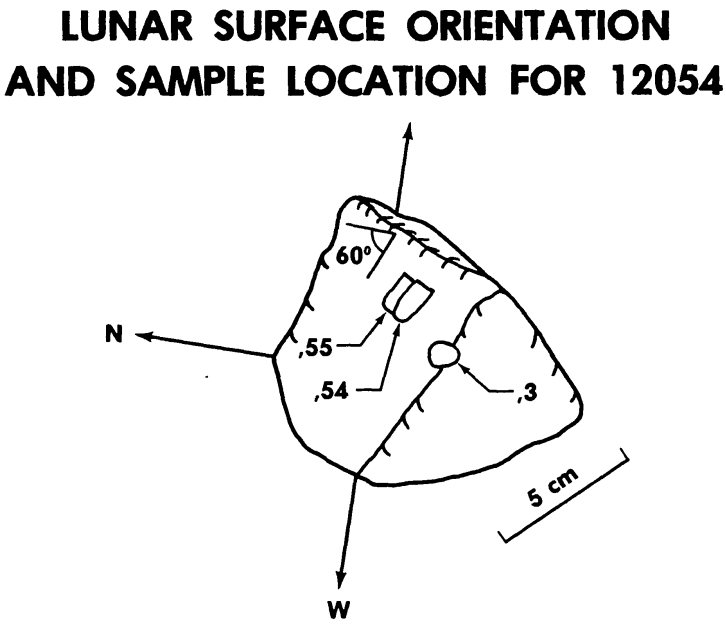

Fig. 1. Graphical representation of the lunar surface orientation of rock 12054 and of the locations of samples 12054,54, 12054,55, and 12054,3. The 60° angle represents the dip of the face sampled and was used in solid angle calculations. The surface depicted was coated with glass.

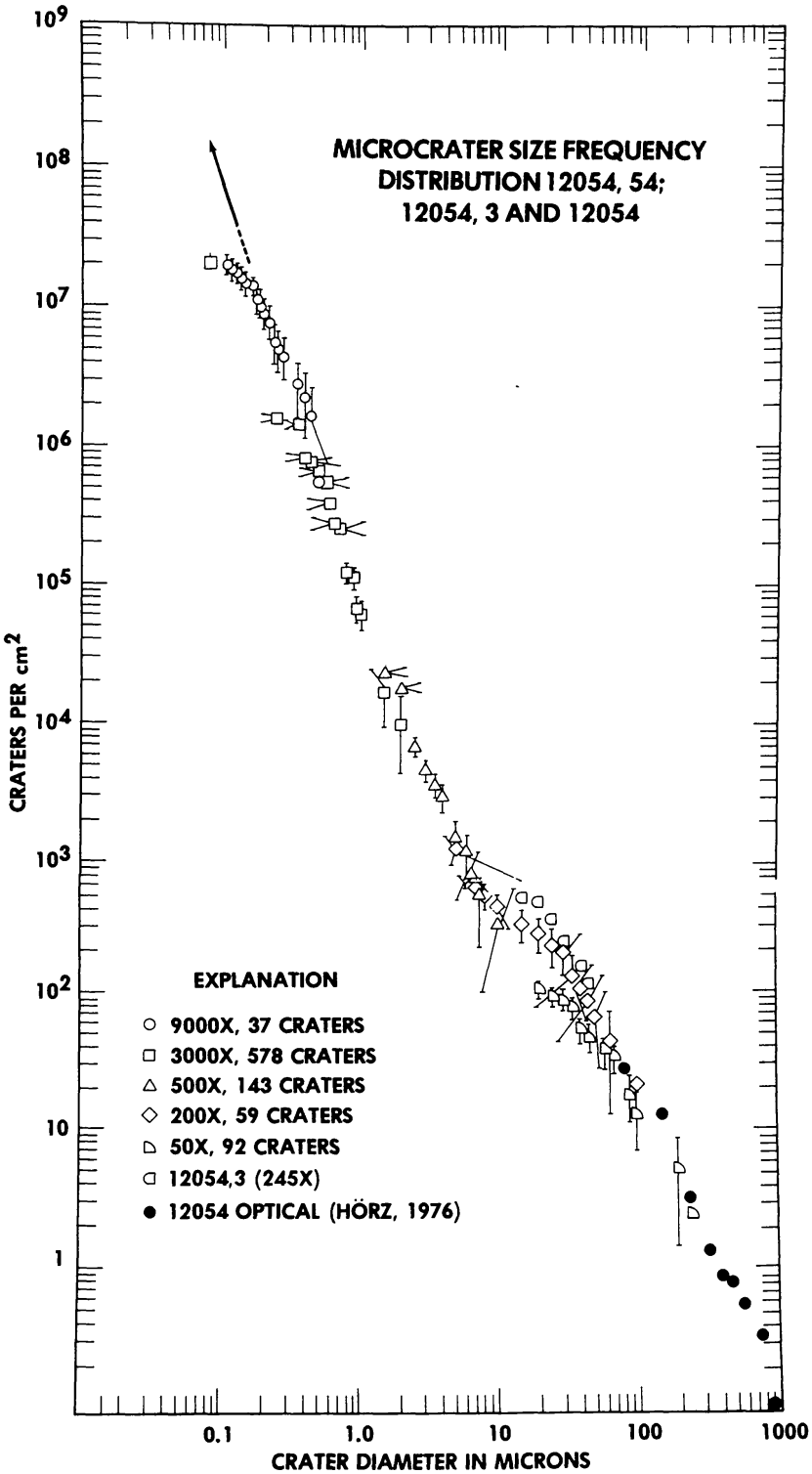

Fig. 2. Crater densities on samples 12054,54 and 12054,3 combined with optical data from the NW face of 12054 as shown in Fig. 1.

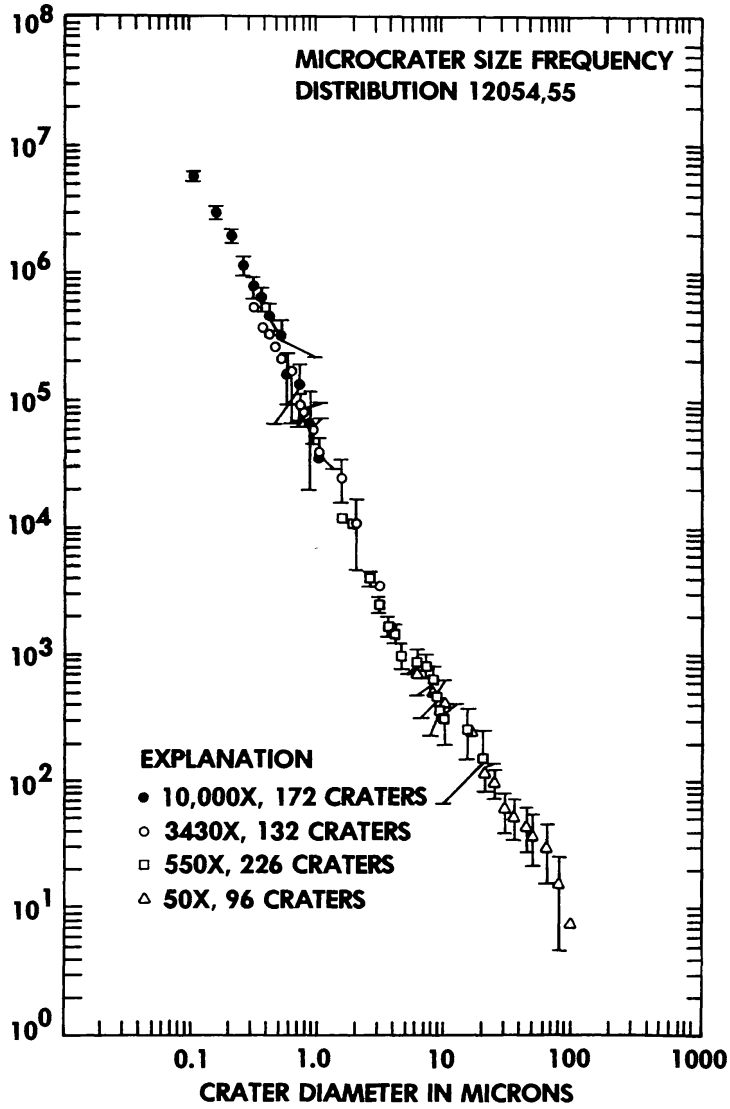

Fig. 3. Microcrater densities on sample 12054,55 determined by SEM techniques.

McDonnell (1977). Figure 4 is a photograph of part of the surface of 12054,54 showing both accretionary features and microcraters. The surface shown in Fig. 4 is typical of our 12054 samples and the picture illustrates the fact that sample surfaces are covered by many generations of glassy debris. Because our samples were cleaned ultrasonically in Freon prior to examination, poorly adhering particles (accreta of McDonnell, 1977) were removed. The surface coverage by accretionary particles as shown in Fig. 4 is therefore less than that of untreated samples.

Accumulation of accretionary particles renews the host surface. Because some craters are covered after production the number of craters observed (on 12054) must be less than the number of craters produced. This effect becomes more important with decreasing crater diameter. For example, the microcrater density distribution measured on 12054,54 bends over for decreasing diameters of less than 0.3 μ, whereas observations of much cleaner surfaces (Brownlee *et*

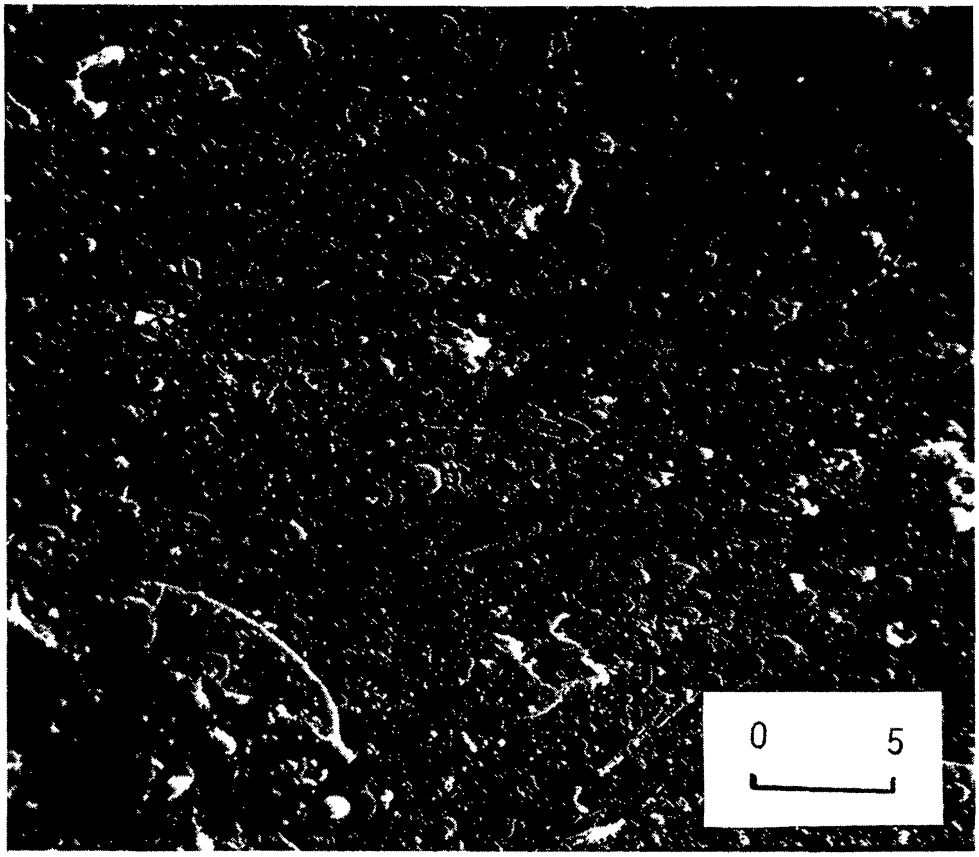

Fig. 4. Glassy particles and "accreta" on the surface of 12054,54, visible at a magnification of 3000×. Approximately 20% of the surface is covered by particles $> 1.5\ \mu$ average dimension. Scale bar is $5\ \mu$.

al., 1975; Blanford *et al.*, 1975) show a constant slope of -2 or steeper extending down to microcrater diameters of $0.1\ \mu$ and smaller. Accordingly, we have extrapolated the submicron crater densities for 12054,54 along the line shown in Fig. 2.

Figure 5 compares the cumulative size frequency distributions of the microcraters on 12054,54 and 12054,55. Microcrater densities on the latter are systematically smaller than on 12054,54 in the interval from 0.1 to $1\ \mu$ diameter although, as shown in Fig. 1, the two samples were close together on the parent rock. This difference may be attributed to variations in the accretionary particle population, which are pronounced (McDonnell, 1977). For larger diameters the two distributions are in better agreement.

In both cases there is an inflection in the microcrater size distribution curves. The inflection is more pronounced for 12054,54 than for 12054,55, but both samples show a flattening of the slope between about 5 and $20\ \mu$ diameter. The curve steepens for diameters less than $5\ \mu$.

Uncorrected microcrater densities on sample 76215,77 are shown in Fig. 6. Also shown are the densities of larger craters counted on the same side of the parent rock on which 76215,77 was located. These measurements were originally

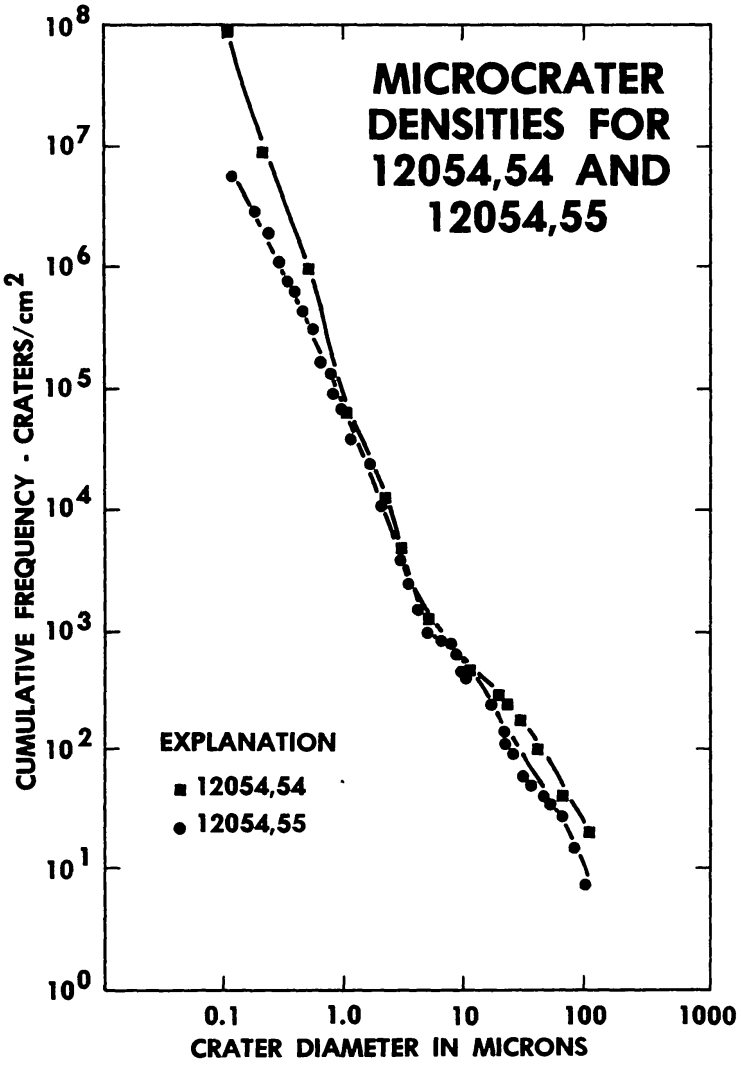

Fig. 5. Comparison of the crater size frequency distribution curves for 12054,54 and ,55. The density of 0.1 μ diameter for ,54 is the extrapolated value as shown in Fig. 2. Absolute densities are plotted without normalization.

reported by Morrison and Zinner (1975). Sample 76215,77 is part of a 2×1 mm anorthite crystal removed from 76215,32. The lunar surface orientation of 76215,32 (and therefore 76215,77) is known precisely (Morrison and Zinner, 1975). The surface of 76215,77 is clean and virtually free of accretionary particles (approximately 1% covered) and no correction of the crater densities is required. This sample therefore provides an independent measurement covering a different exposure time than 12054 (see below), of the slope of the crater distribution curve for micron and submicron diameter craters. There are too few craters of $> 100\ \mu$, however, on 76215,77 to yield measurements with adequate statistics for larger diameters.

Densities of submicron and $> 100\ \mu$ diameter craters from 12054,54 and 12054 (Hörz, 1976 pers. comm.) are also plotted in Fig. 6 and can be compared to the data from 76215. For the latter the number of craters of 0.1 μ diameter or

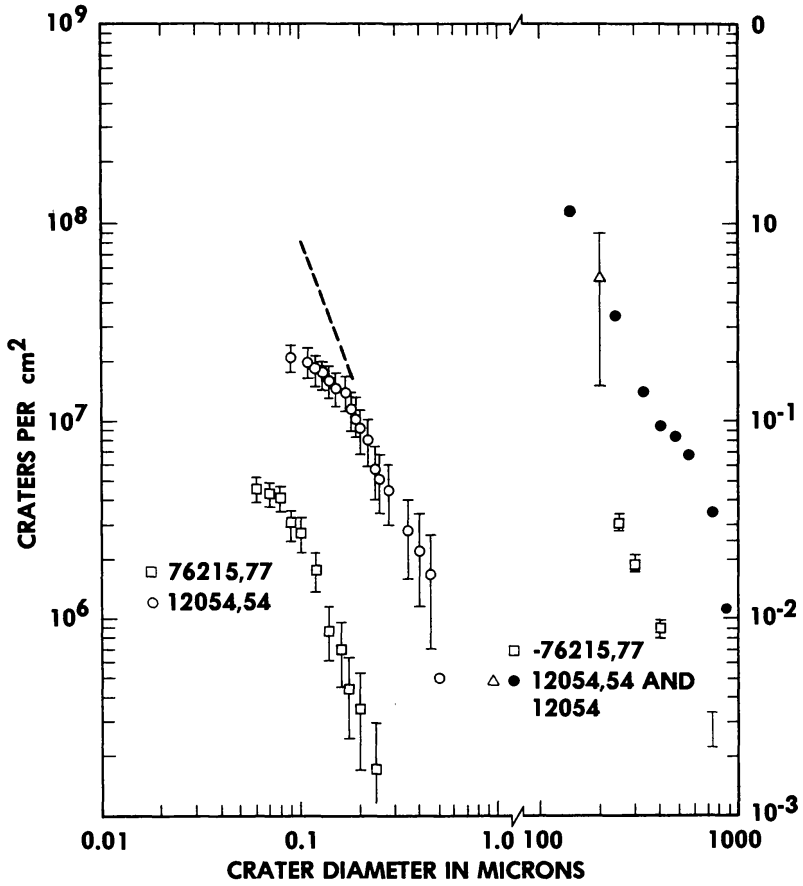

Fig. 6. Crater densities on 76215 and 12054. On the left of the figure are the submicron crater densities for both rocks. On the right are the $> 100\ \mu$ diameter craters for both samples. Solid circles for 12054 represent the data of Hörz (1976), and the open triangle is our SEM data for 12054. Open squares are optical data for 76215.

larger is 2.7×10^6 per cm^2, that of craters of $500\ \mu$ diameter or larger is 0.06 per cm^2. The ratio of the densities of these two sizes is thus 4.5×10^7, but statistics are poor for the larger craters because only 13 were counted. For 12054,54 the minimum density of $0.1\ \mu$ diameter craters produced should be the extrapolated density (Fig. 2) of 8×10^7 per cm^2. The number of $500\ \mu$ diameter or larger craters on the same side of the rock is 0.8 per cm^2 (Fig. 5) giving a ratio of 1×10^8.

Cosmic Ray Tracks

Track density versus depth profiles for 76215,77 and 12054,3 are shown in Fig. 7. Track densities at depths less than about $70\ \mu$ in 12054,3 could not be measured because of the glass coating, but several feldspar crystals were observed trapped in the glass near the surface of 12054,54. Preliminary counts of track densities in these crystals show agreement within a factor of two at depths of $10–20\ \mu$ with densities expected from the 12054,3 measurements.

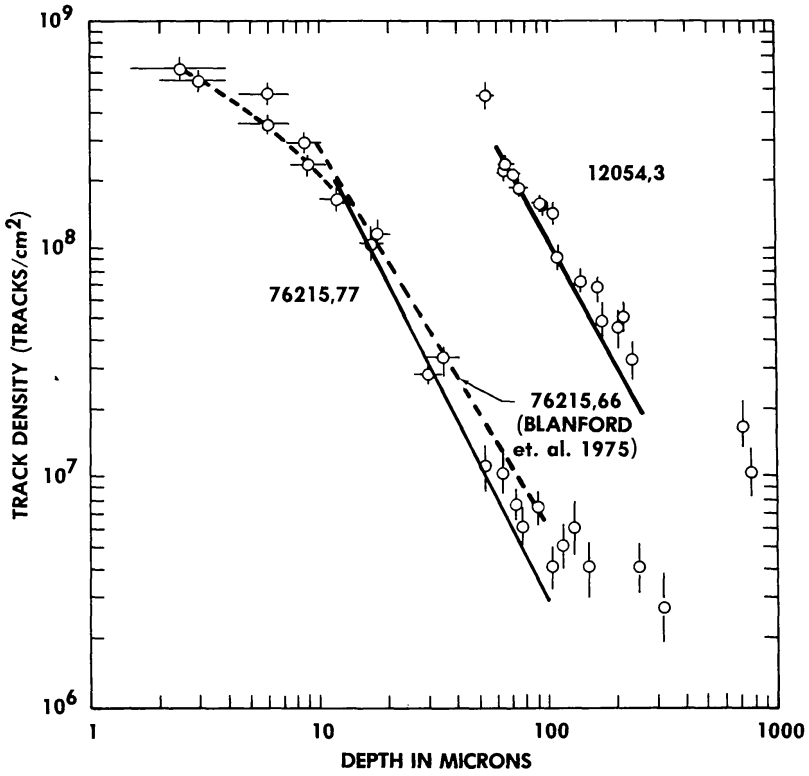

Fig. 7. Track density versus depth profiles for 76215,77 and 12054,3. Data for 76215 from Blanford *et al.* (1975) is also shown. For both rocks, the solid line represents the solar flare track density after correcting for the background of galactic tracks. The observable depth in the case of 12054 was limited by the glass coating.

Both the 76215 and 12054 samples show steep slopes of the track density versus depth profiles characteristic of solar flare produced tracks. The steep slope extends to a depth of approximately 80 μ for 76215,77 and to approximately 300 μ for 12054. At these depths the background of tracks produced by galactic cosmic rays becomes noticeable. The solid lines in Fig. 7 correct for this background. With this background correction the slopes of the track density profiles are -1.97 and -1.86 for 76215 and 12054 respectively. Background track densities for 12054 vary by approximately a factor of two from place to place but average about 2×10^7 tracks per cm^2 through to the bottom of the rock as it sat on the lunar surface. The variations are the result of the less than ideal condition of 12054 for track etching work. The rock was heavily shocked and tracks usually could be observed only in small areas which did not break up in the etching process. A density of 2×10^7 tracks per cm^2 throughout the rock indicates an irradiation history for 12054 in the upper part of the regolith prior to its last stage surface exposure. The exposure history of 76215 has been described by Blanford *et al.* (1975) and Morrison and Zinner (1975).

Also shown in Fig. 7 is the track density profile for 76215,66 obtained by Blanford *et al.* (1975). Exposure geometries for this sample and 76215,77 were the same.

Discussion

Crater size distribution

Data from 12054, from our work and other studies (Hörz, 1972; Hörz *et al.*, 1974; Mandeville, 1977) provide a cumulative crater size frequency distribution over approximately four orders of magnitude in crater size. 12054 is the first lunar rock measured for which the data spans such a range with adequate statistics for all size intervals.

The distribution has several parts. The slope (of crater density versus diameter on a log-log plot) is -2.5 to -2.8 from crater diameters of 0.1 μ to diameters of 5 to 7 μ. The steeper slope is from 12054,54 (Fig. 2) where the surface appears to have been less affected by accretionary particles. These slopes are steeper than the -2 slope assumed by Morrison and Zinner (1976) and obtained by Fechtig *et al.* (1975), but comparable to the slope of -2 to -3 determined by Brownlee *et al.* (1975) for sample 60095. At crater diameters of about 5 μ for 12054,55 and 7 μ for 12054,54, the distribution changes. The slope flattens to values of -0.7 to -0.8 approximately, then steepens to approximately -1.7 at crater diameters of 10 and 25 μ for 12054,55 and 12054,54 respectively. It then progressively steepens to values of -2.5 to -3 for craters from approximately 200 to 1500 μ diameter (Hörz, 1976, Hartung *et al.*, 1972). These values are smaller than the value of -3.75 over the same range obtained by Fechtig *et al.* (1975) from several rocks, many of which were in steady state. In this case, the steepening of the curve to a slope of -3.75 may be caused by the "selection effect" defined by Hartung *et al.* (1972) and may not be an accurate representation of the production distribution.

We emphasize that the data in Figs. 2 and 3 are not normalized. At a single magnification setting of 550× in Fig. 3 for example, the bimodal form of the distribution is apparent. This rules out crater recognition problems or crater shielding by accretionary particles as causes for the bimodality. In the case of 12054,54 measurements at 200 and 500× were repeated and over 200 additional craters were counted with identical results. The presence of the flexure therefore is not caused by counting errors although the precise diameter range over which the bend occurs may be. The data of Mandeville (1977) show a bend in the distribution at a crater diameter of 10 μ, but the slope for the distribution of smaller craters (1–10 μ) in this case is less than -1.5 and significantly shallower than ours over the same range. We observe about 7 times more 1.0 μ craters for every 100 μ diameter crater than Mandeville (1977). The data of Fectig *et al.* (1975) show a bimodal distribution with a slope of -1 between crater diameters of 2 and 200 μ. Their distribution curve was based upon many normalized curve segments obtained from different rocks, only one of which (15205) provided data over the whole size range. More recent work on 15205 (Comstock *et al.*, 1977) suggests that the samples of 15205 examined were covered by a dust coating which may have contributed to flattening of the slope by filtering out smaller projectiles.

The data from 12054 shows a more pronounced bimodality than the distribution of our earlier model (Morrison and Zinner, 1976). The latter is a composite curve based upon rock 76215 for the submicron and $> 250\ \mu$ diameter crater populations, plus data from samples 15015 and 15017 (Morrison *et al.*, 1973) and 15286 (Brownlee *et al.*, 1973) for the intermediate crater sizes. All of these samples had uneroded surfaces with no apparent dust covering. The ratio of 0.1 to 500 μ diameter craters is 3.5×10^7 to 1.5×10^8 for the earlier model (Morrison and Zinner, 1976) comparable to the ratio of 1×10^8 for 12054. The equivalent ratio for the data of Fechtig *et al.* (1975) is 1.7×10^6. Our earlier model, however, is incorrect for the intermediate (10–100 μ) diameter craters possibly because of the difficulties in normalizing curve segments from several rocks. The data for 12054 and 60095 (Brownlee *et al.*, 1975) are superior because normalization is not required. The crater frequency distribution from 12054 and 60095 therefore appear to be the most reliable as well as the most complete.

The bimodal form of the crater frequency distribution reflects a bimodal micrometeorite complex (Hörz *et al.*, 1975). Models for a bimodal micrometeorite population have been postulated by a number of workers (e.g., Dohnanyi, 1970; Fechtig *et al.*, 1974, 1975, and most recently Dohnanyi, 1976). These models all suggest that the larger craters ($> 5.7\ \mu$ in our case) represent particles spiraling into the sun, whereas the smaller craters are produced by particles propelled away from the sun by radiation pressure. The latter represent the beta meteoroids of Zook and Berg (1975) produced predominantly by fragmentation of larger parent particles. Dohnanyi (1976) developed a quantitative model based upon this hypothesis to reproduce the bimodal crater size meteoroid more frequency distribution of Fechtig *et al.* (1974).

Our results do not contradict this model, but the higher ratio of small to large craters (or particles) that we observe, compared to Fechtig *et al.* (1974), indicates a more efficient production of beta-micrometeoroids by approximately an order of magnitude. Such an increase is well within the range of parameters selected by Dohnanyi (1976).

Solar flare production rate

A persistent problem in the study of processes affecting the lunar surface has been the characterization and calibration of the solar flare particle flux, largely because of the lack of suitable samples. Several track production rates exist (e.g., Hartung and Storzer, 1974; Hutcheon *et al.*, 1974; Blanford *et al.*, 1975). We prefer the Blanford *et al.* (1975) model for the following reasons. First, the Blanford *et al.* (1975) track production rate was calibrated by an independent krypton isotope measurement (Marti, pers. comm. as cited by Blanford *et al.*, 1975) of the exposure age of the sample in which track measurements were made. Secondly, the slope of the track density versus depth profile of Blanford *et al.* (1975) agrees with our own measurements (Morrison and Zinner, 1975, 1976). These slopes are not as steep as the profile of Surveyor III (Crozaz and Walker, 1971; Fleischer *et al.*, 1971; Price *et al.*, 1971) indeed, no track profiles in

crystalline material have been observed to be as steep as the Surveyor III profile over the whole range. Profiles in lunar glasses (Storzer *et al.*, 1973; Hartung and Storzer, 1975) with slopes of –2.5, equivalent to Surveyor III, have been called into question by the results of Comstock and Hartung (1977). The data from 12054 and 76215 offer an opportunity to check the Blanford *et al.* (1975) track production rate model.

Using the track production rate of Blanford *et al.* (1975) we calculate the exposure age of 12054 to be $1.75 \pm 0.25 \times 10^5$ yr. Some check on this value, and thus indirectly on the Blanford production rate is possible through the ^{26}Al measurements of Schonfeld (pers. comm.). Schonfeld measured a total ^{26}Al activity of 53 ± 10 dpm/kg in 12054 (see also O'Kelley *et al.*, 1971), and a 10% difference was detected between the top or exposed surfaces and the bottom or shielded surface. Schonfeld (pers. comm.) suggests that this difference indicates irradiation near or on the lunar surface prior to the most recent surface exposure. Our observations of track densities of $1-2 \times 10^7$ per cm^2 in the interior of 12054 verify the exposure of 12054 to cosmic rays while buried a short distance beneath the lunar surface as postulated by Schonfeld. A pre-irradiation episode of 12054 is also indicated by the noble gas measurements of Bogard *et al.* (1971) which yield a galactic cosmic ray exposure age of 1.5×10^8 yr. Because of the rapid fall-off of the galactic cosmic ray spectrum the pre-surface exposure episode shown by the ^{26}Al data could not have taken place at depths of more than 20 cm and most likely occurred at a depth of 5–10 cm.

With these data, and the new chemical analysis of 12054 by Rhodes *et al.* (1977), an exposure age based on ^{24}Al can be calculated for 12054. The result is $1.60 \pm 0.5 \times 10^5$ yr (Schonfeld, pers. comm) for a 2-stage history. (An assumption of no prior irradiation, which is ruled out, results in an exposure age of $2.40 \pm 0.8 \times 10^5$ yr) This measurement is in excellent agreement with the track exposure age of $1.75 \pm 0.25 \times 10^5$.

A second calibration of the track production rate is offered by the studies of 76215,77 (Fig. 6), and the work of Zinner *et al.* (1977), and Blanford *et al.* (1975) on 76215,77 and other samples of rock 76215. Our track data for 76215,77 indicate an exposure age of approximately 16,000 yr with the Blanford *et al.* (1975) track production rate. Zinner *et al.* (1977) and Zinner *et al.* (this volume) have determined the surface concentrations of Mg and Fe on this same sample, and argue that these metals are implanted solar wind ions. Using the concentrations observed, they calculate solar wind exposure ages for 76215,77 to be 2.5×10^4 yr for Mg and 2.1×10^4 yr for Fe in reasonable agreement with the track age of 76215,77. These ages assume the Cameron abundances for solar wind species.

Furthermore, the ratio of tracks to pits (of 0.1μ diameter) is the same for 76215,77 and our samples of 12054, and the ratio of Mg ion concentration to 0.1 μ diameter pits is shown by Zinner *et al.* (1977) to be approximately the same for 76215,77 and 76215,91. This consistency between the results of three methods of measuring exposure times on the lunar surface thus confirms the Blanford *et al.* (1975) track production rate to the exclusion of the Hutcheon *et*

al. (1974) rate. (See however Hutcheon (1976) on the point of intercalibration of track measurements between different laboratories.)

Exposure age calculations based upon solar fluxes assume that the sun has been relatively constant. We have previously introduced (Morrison and Zinner, 1975; Morrison and Zinner, 1976a, b) the ratio of the cumulative density of craters greater than or equal to 0.1 μ diameter to the track density at 100 μ depth, both observed in the same sample, as a measure of the relative rates of crater and track production. Data from previous measurements and the measurements reported here are shown in Fig. 8. The track densities and crater densities plotted are observed densities not adjusted for exposure age or solid angle. In all four cases tracks were measured in a plane normal to the cratered surface. The ratio of both densities is the same for all four samples within error limits showing no relative change in either process over the time sampled. Because both processes would have to change sympathetically to maintain a constant ratio, the data suggest that both have been constant. Figure 8 also shows exposure ages calculated for the four samples. Such calculations necessarily take into account the solid angle for each individual exposure geometry. The results for each sample give the same microcrater production over time periods from about 16000 to 5.3×10^5 yr. The observation of a constant ratio

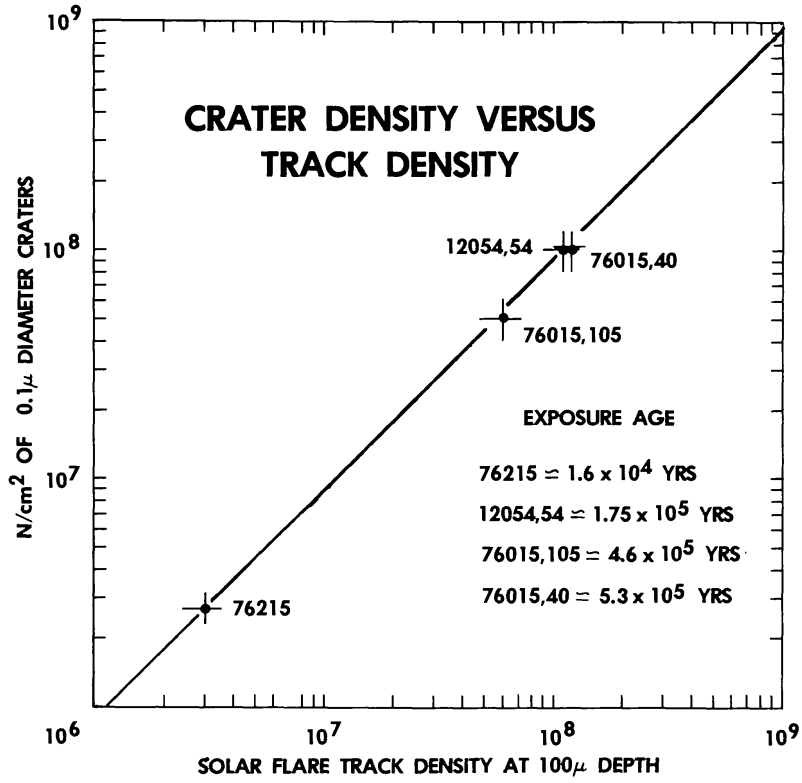

Fig. 8. Plot of density of 0.1 μ diameter or larger craters versus observed track density at 100 μ depth. The latter is uncorrected except for background tracks. Data for the 76015 samples is from Morrison and Zinner, 1975, the others from this work. Also shown are the exposure ages calculated for the samples plotted.

between crater and track densities plus the correspondence between our track data and the solar wind measurements of Zinner *et al.* (this volume), is good evidence for a lack of variation in the output of solar wind and solar flare particles within the limits of our measurements. Nishiizuma *et al.* (1976), Reedy (1977), and Bhandari (1977) draw the same conclusion from considerations of solar flare proton fluxes. These data do not exclude short term solar variations as postulated by Eddy (1976) from historical sun spot data.

These results disagree with the conclusions of Zook *et al.* (1976, 1977), who postulate a highly probable variation in the solar flare track production rate, perhaps by as much as a factor of 50, averaged over 1000 yr periods during the last 16,000 yr. This conclusion was based upon an analysis of track and crater data for sample 15205 obtained by Hartung and Storzer (1975). More recent work on the same sample, however, by Comstock and Hartung (1977) and Hartung *et al.* (1977) has refuted the data which Zook *et al.* (1976, 1977) considered.

Solar wind erosion

The surface of 76215,77 was exposed to micrometeorites, solar flare particles and the solar wind. The crater densities at 0.1 μ diameter show no bending of the slope as might be expected if solar wind erosion occurred at a high rate. Estimates of solar wind erosion vary by more than an order of magnitude from about 0.025 to 0.5 Å/yr (McDonnell and Ashworth, 1974; Bibring *et al.*, 1977; McDonnell, 1977). The larger rate would imply a removal of 0.8 μ (8000 Å) from the surface of 76215,77. Some features of the surface suggest that this did not occur. Figure 9 shows filaments of anorthite welded to the surface of 76215,77. The filaments represent cleavage fragments sheared from the anorthite crystal surface during the passage of the shock wave generated in the impact event which removed 76215 from its parent boulder (Morrison and Zinner, 1975; ALGIT, 1973). A part of the surface of the crystal from which 76215,77 was removed consists of ultramylonite, also indicating some heating of parts of the surface during the impact generated shearing. The filaments drape over the topography (e.g., at A, Fig. 9) of the underlying crystal indicating that they were hot enough to be plastically deformed. We conclude that the filaments are as old as the host surface.

The filaments are from 0.2 to 0.1 μ wide and from approximately 0.1 μ to 500 Å or less thick. The filaments at A, C, and D (Fig. 9) have uniform dimensions throughout their length. Such uniformity of shape would not be observed if the filaments were erosional remnants of forms originally eight times larger approximately as required by an erosion rate of 0.5 Å/yr (Bibring *et al.* 1977). Furthermore, removal of approximately 1000 to 1500 Å of surfaces of 76215,77 in the ion microprobe (Zinner *et al.*, 1976) eradicated *all* the detailed features seen in Fig. 9. From the presence of these features we thus can set an upper limit of 0.03 Å/yr on the erosion rate from solar wind sputtering. In principle, one could also use the size frequency distribution of submicron craters for an erosion rate estimate. Solar wind erosion would result in a flattening of

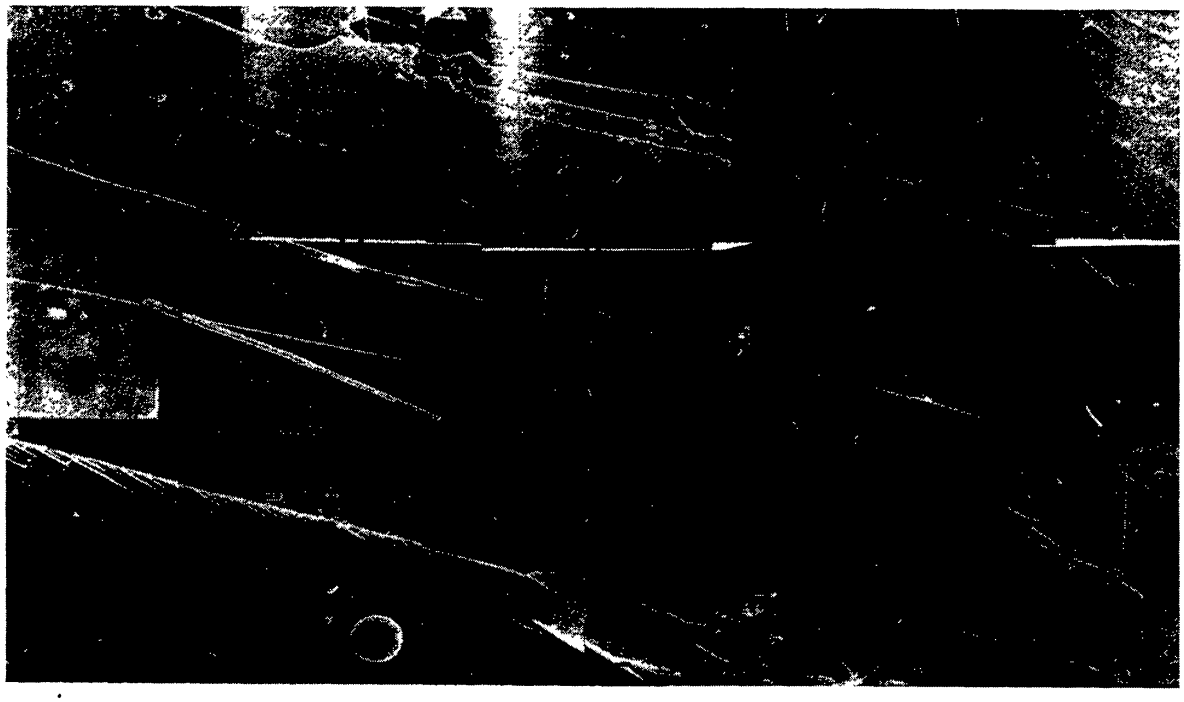

Fig. 9. SEM photograph of the surface of an anorthite crystal from 76215 at a magnification of about 6000×. Scale bar corresponds to 5 μ. Filaments are shown at A, B, C, D, and E. The filament at D has buckled, possibly because of expansion. The filaments at B, C, and E are $\leq$ 500 Å thick. All of the features shown were removed by sputtering in the ion probe.

the crater density slope for small crater diameters. No such flattening is observed of the microcrater size distribution measured on 76215,77 (Fig. 5) when compared to the distribution from a surface which was not exposed to the solar wind (76015,40; Morrison and Zinner, 1975). This observation leads to an upper limit estimate of the solar wind erosion rate which is approximately the same as that obtained from the filaments. However, this estimate rests on the assumption that the microcrater size distribution is the same for different periods and for surfaces of different orientations (pointing in and out of the ecliptic). Since, furthermore, unlike the filaments, not all craters are as old as the host surface, the value based on the observation of filaments is more certain. We thus conclude that solar wind erosion on surfaces like 76215,77 proceeds at a rate of less than 0.03 Å/yr.

Cratering rates

From the cumulative crater densities and the track data from 12054 we can calculate the production rate of microcraters in the size range shown in Figs. 2, 3, and 5. Our results are given in Fig. 10. The crater production rate is normalized to an exposure time of one year. The new data compare favorably with our earlier model (Morrison and Zinner, 1976) for the submicron and

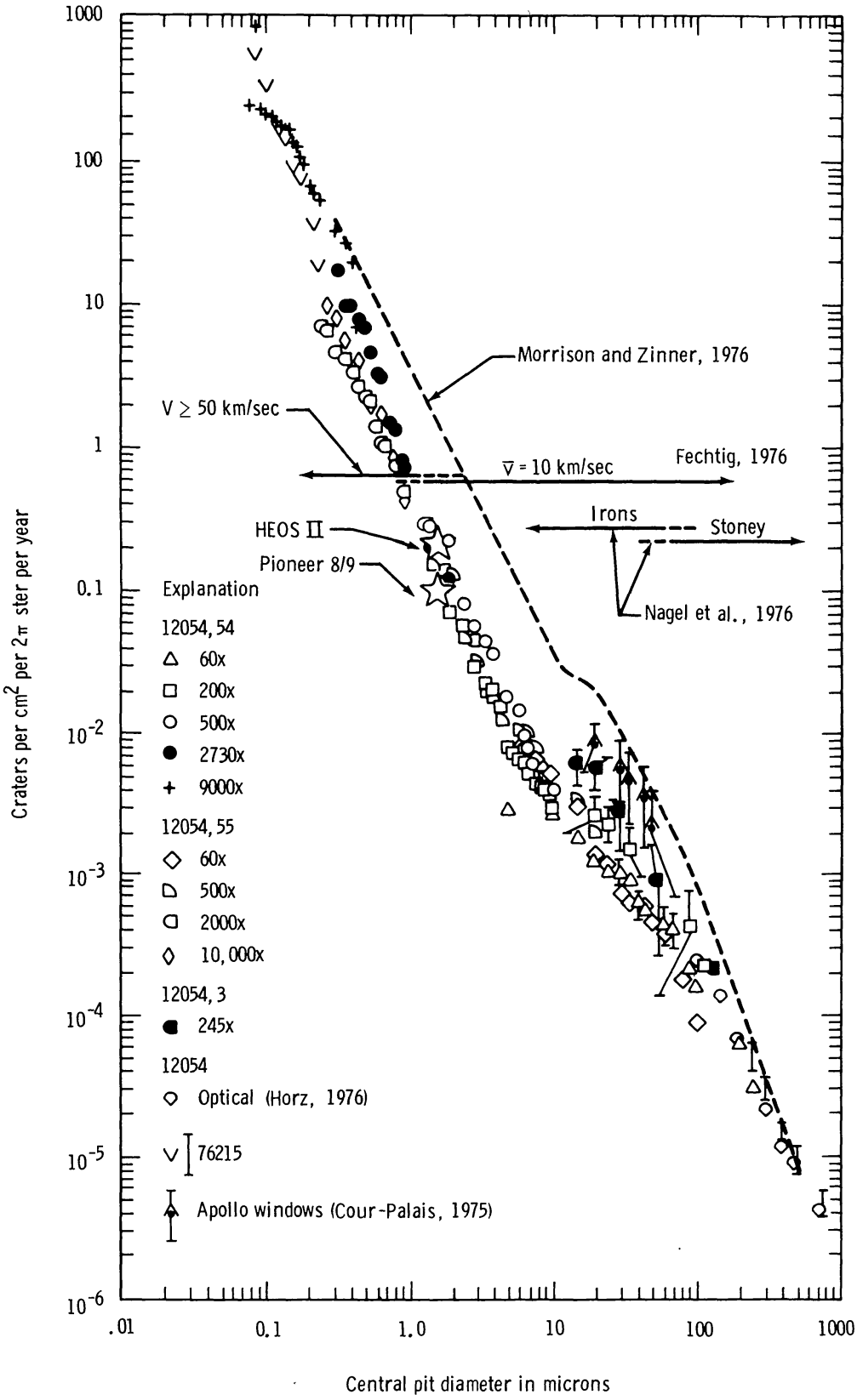

Fig. 10. The crater production rate determined from 12054 and 76215 compared to satellite data. Crater diameter refers to the central pit. The dotted line shows the distribution and cratering rate of Morrison and Zinner, 1976.

$> 100\ \mu$ craters but there are significant discrepancies for the intermediate crater diameters. The production rates of our earlier model in this size range were based on a combination of data obtained from different rocks which also suffered in some cases from poor statistics as previously pointed out. The new curve has the advantage of being based on adequate data which were obtained from a single rock surface.

Figure 10 also shows other meteoroid flux data obtained independently by other investigators. The curve representing the Apollo window meteoroid data (Cour-Palais, 1975) is derived from the actual central pit measurements provided by Cour-Palais (pers. comm.) rather than from the meteoroid flux data which are given in terms of the meteorite mass in the published work (Cour-Palais, 1975). We believe it to be simpler to directly compare crater size measurements and not go through the conversion from meteorite masses (originally derived from crater sizes) back to crater sizes again. Further, since there is a sizeable uncertainty in this conversion between crater sizes and dust particle masses (e.g., Hörz *et al.*, 1975), the application of different size-mass calibration relations can lead to errors (Zook *et al.*, 1977).

Ten craters were measured on the Apollo windows but central pit measurements for seven only are available—all with central pits equal to or greater than $20\ \mu$. The remaining three had spall diameters of $25\ \mu$ (2 ea.) and $65\ \mu$ (Cour-Palais, 1974, Table 1). Given the range of spall to pit diameters of 3.7 to 6.5 measured on the windows (Cour-Palais, unpublished data) these three craters must have central pits much less than $20\ \mu$ diameter. Therefore their exclusion does not affect the window data plotted in Fig. 10. These data points were calculated with a time-area constant of $14.32 \times 10^5\ \mathrm{cm}^{-2}\ \mathrm{sec}^{-1}$, and the result reduced by a correction factor for earth focusing of 0.52 following Cour-Palais (1974). The flux so calculated is higher than that determined from our lunar rock data by about a factor of 3. In evaluating this difference, it is important to consider the experimental settings. Six of the craters on the windows were produced in earth orbit (5 on Apollo 7 and 1 on Apollo 9), whereas only one was observed (from Apollo 13 mission which went around the moon) which may have been produced far from earth. Fechtig (1976) has re-emphasized the point that an enhanced dust flux near the earth has been measured. Data taken by the Heos II satellite, in an elliptic orbit around the earth, show an enhancement of a factor of 5 in random particle events detected near earth ($< 67{,}000$ km) compared to the number of events detected in interplanetary space. If particles in swarms and groups also measured by Heos II are considered, then the near earth flux is more than an order of magnitude higher than the flux in interplanetary space. Bedford *et al.* (1975) have re-appraised Prospero data and the results agree with the Heos II observations. Consequently, the Apollo window data should indicate a higher flux than lunar sample data by a factor of 5 or more, and such is the case, and the two results cannot be said to be in disagreement. Further, before application of the Apollo window results to lunar problems (e.g., as a microcrater clock, Zook *et al.*, 1977) a correction for this flux difference must be made.

The Skylab S-149 experiment measured the microcrater production rate in near-earth orbit. Data obtained from this experiment shows also an enhancement of the dust flux near the earth. This is shown by Nagel *et al.* (1976), who measured 49 craters and divided them into two groups. The first group consists of 5 craters between 1 and 30 μ diameter which were found on various detectors, and the second consists of 44 craters between 1 and 4 μ diameter clustered on one detector. The latter group is interpreted by Nagel *et al.* (1976) to result from the fragmentation of a single larger micrometeorite, a process which leads to near-earth enhancement (Fechtig, 1976). This interpretation yields a total of six particles (craters) and a flux consistent with our results, however if the 44 craters are interpreted to be formed by unrelated particles then the flux calculated is 100 times higher (Nagel *et al.*, 1976). These results support the hypothesis of a near-earth enhancement of the dust flux and demonstrate that data acquired in near-earth orbit cannot be compared directly to lunar data.

The Heos II and Pioneer 8 and 9 satellites have measured interplanetary dust fluxes at 1 a.u., and it is of interest to compare these contemporary data with the long term record from lunar rocks. In Fig. 10, we have plotted the satellite measured fluxes, in the apex direction, of 10^{-12} g particles converted to a 2π exposure geometry. In converting micrometeorite mass to crater diameter, we have used the calibration of Mandeville and Vedder (1971). A comparison between satellite and lunar data cannot be made directly without considering the properties of both detectors. The flux in the apex direction measured by the satellites is higher than the flux in other directions. Hörz *et al.* (1975) and Hoffman *et al.* (1975) point out that, because the moon spins, lunar rock detectors are exposed to the apex flux only part of the time and the flux recorded should be 3 times less than the apex flux measured by the satellites. An additional correction factor for comparison between particle fluxes obtained from lunar rocks and satellite detectors is introduced by the fact that satellite measurements are normalized to a 2π s.r. detector geometry under the assumption of an isotropic dust flux. Since, in fact, this flux is highly anisotropic, this normalization procedure overestimates the flux value measured by Heos II by a factor of about 3 (Hoffman *et al.*, 1975). Thus, Hoffman *et al.* (1975) conclude that normalized satellite apex fluxes should be 6 to 12 times higher than fluxes derived from lunar rocks. Accordingly, we have reduced the published values for Heos II (Hoffman *et al.*, 1975) and Pioneer 8/9 (McDonnell *et al.*, 1975) by a factor of 6 and plotted these reduced flux values in Fig. 10. Not considered, however, are possible variations in the physical properties and the velocity distributions of micrometeorites with particle size. These are indicated in Fig. 10. (Nagel *et al.* (1976) show, on the basis of crater diameter to depth ratio measurements, that higher density particles (e.g., irons) become more abundant with decreasing particle (or crater) diameter. Fectig *et al.* (1976) interpret Heos II data as indicating very high velocities for smaller particles ($\leqslant 1\ \mu$ diameter) of probable beta meteoroid origin, but a velocity of about 10 km/sec for larger particles. The calibration of Mandeville and Vedder (1971) assumes a density of 3 g/cm^3 and a velocity of 20 km/sec. Taken together, the above observations

would result in a higher micrometeorite mass flux derived from lunar microcrater measurements for particles with velocities less than 20 km/sec, and a lower flux for particles with velocities greater than 20 km/sec and clearly must imply considerable uncertainty when comparing crater diameter to micrometeorite mass measurements. It appears, however, that there is no major discrepancy between our data from lunar rocks 12054 and 76215, averaging the micrometeorite flux for long periods of time, and the contemporary satellite data collected at 1 a.u.

CONCLUSIONS

1. The size frequency distribution of micrometeorites is bimodal as first shown clearly by Schneider *et al.* (1973). The ratio of the density of 0.1 μ diameter or larger craters to the density of 500 μ and larger craters from our data is 5×10^7 to 1×10^8, significantly higher than the ratio of about 1.7×10^6 from the distribution of Fechtig *et al.* (1975).
2. Using the Blanford *et al.* (1975) track production profile we calculate an exposure age for 12054 of $1.75 + 0.25 \times 10^5$ yr. Galactic track densities in the interior of 12054 indicate exposure of 12054 to cosmic rays before it was implaced on the lunar surface about 1.75×10^5 yr ago. This prior irradiation probably took place at a depth of 5–10 cm. Schonfeld (pers. comm.) calculates an exposure age of $1.60 \pm 0.5 \times 10^5$ yr for 12054 from ^{26}Al data assuming a prior irradiation.
3. The solar flare track exposure age of 76215,77 is approximately 16,000 yr using the Blanford *et al.*, 1975 track production rate. This age agrees with the exposure age for the same surface calculated by Zinner *et al.* (1977) and Zinner *et al.* (this volume) from solar wind Mg and Fe abundances.
4. The agreement between exposure ages calculated from solar wind, solar flare tracks, and ^{26}Al measurements confirm the Blanford *et al.* (1975) track production model, and indicate no variation in solar activity within measurement limits over a 2 m.y. period.
5. The crater production rate and the micrometeoroid fluxes inferred therefrom are the same for both 76215 and 12054. The cratering rate for submicron diameter craters from these samples also agrees with our previous results (Morrison and Zinner, 1976) from surfaces exposed for longer periods of time. The data also agree with the HEOS II and Pioneer 8 and 9 measurements of the interplanetary dust flux at 1 a.u., and we conclude that there has been no variation within error limits of the dust flux for 5×10^5 yr.
6. The submicron-sized anorthite filaments present on the surface of 76215,77 throughout its 16,000 yr exposure to the solar wind limit solar wind erosion of anorthite to less than or equal to 0.03 Å/yr. Submicron crater distributions lead to the same result but with less certainty.

References

ALGIT (Apollo Lunar Geology Investigation Team) U.S. Geological Survey (1973) Preliminary analysis of the Apollo 17 site. *U.S. Geol. Survey, Interagency Rept: Astrogeology* No. 72. 211 pp.

Bibring J. P., Chaumont J., Dran J. C., Lalu F., Langevin Y., Maurette M., and Vassent B. (1977) Solar wind erosion of lunar dust grains. A progress report (abstract). In *Lunar Science VIII*, p. 106–109. Lunar Science Institute, Houston.

Bhandari N. (1977) Solar flare induced Al^{26} in short exposure age rocks (abstract). In *Lunar Science VIII*, p. 100–102. The Lunar Science Institute, Houston.

Blanford G. E., Fruland R. M., McKay D. S., and Morrison D. A. (1974) Lunar surface phenomena: Solar flare track gradients, microcraters, and accretionary particles. *Proc. Lunar Sci. Conf. 5th*, p. 2501–2526.

Blanford G. E., Fruland R. M., and Morrison D. A. (1975) Long term differential energy spectrum for solar flare iron-group particles. *Proc. Lunar Sci. Conf. 6th*, p. 3557–3576.

Bogard D., Funkhouser J. G., Schaeffer O. A., and Zahringer J. (1971) Noble gas abundances in lunar material-cosmic ray spallation products and radiation ages from the Sea of Tranquility and the Ocean of Storms. *J. Geophys. Res.* **76**, 2757–2779.

Brownlee D. E., Hörz F., Hartung J. B., and Gault D. E. (1975) Density, chemistry and size distribution of interplanetary dust. *Proc. Lunar Sci. Conf. 6th*, p. 3409–3416.

Comstock G. and Hartung J. (1977) Found: Solar iron-group tracks in microcrater glass (abstract). In *Lunar Science VIII*, p. 205–206. The Lunar Science Institute, Houston.

Cour-Palais B. (1975) The current micrometeoroid flux at the moon for masses $\leqslant 10^{-7}$ g from the Apollo window and Surveyor 3 TV camera results. *Proc. Lunar Sci. Conf. 5th*, p. 2451–2462.

Crozaz G. and Walker R. M. (1971) Solar particle tracks in glass from the Surveyor 3 spacecraft. *Science* **171**, 1237–1239.

Dohnanyi J. (1970) On the origin and distribution of micrometeoroids. *J. Geophys. Res.* **75**, 3468–3493.

Dohnanyi J. (1976) Flux of hyperbolic meteoroids, In *Interplanetary Dust and Zodiacal Light* (H. Elsaesser and H. Fechtig, eds.), p. 170–180. Springer-Verlag, New York.

Eddy J. A. (1976) The Maunder minimum. *Science* **192**, 1189–1202.

Fechtig H. (1976) *In situ* records of interplanetary dust particles: Methods and results. In *Interplanetary Dust and Zodiacal Light* (H. Elsaesser and H. Fechtig, eds.), p. 143–158. Springer-Verlag, New York.

Fechtig H., Gentner W., Hartung J. B., Nagel K., Neukum G., Schneider E., and Storzer D. (1975) Microcraters on lunar samples. In *Proc. Sov.-Amer. Conf. on Cosmochemistry of the Moon and Planets (Moscow)*. NASA SP-370. In press.

Fechtig. H., Hartung J. B., Nagel K., and Neukum G. (1974) Lunar microcrater studies, derived meteoroid fluxes, and comparison with satellite-borne experiments. *Proc. Lunar Sci. Conf. 5th*, p. 2463–2474.

Fleischer R. L., Hart H. R., Jr., and Comstock G. M. (1971) Very heavy solar cosmic rays: Energy spectrum and implications for lunar erosion. *Science* **171**, 1240–1241.

Hartung J. B., Breig J. J., and Comstock G. M. (1977) Microcrater studies on 60015 do not support time variation of meteoroid flux (abstract). In *Lunar Science VIII*, p. 406–408. The Lunar Science Institute, Houston.

Hartung J. B., Hörz F., Aitken K. F., Gault D. E., and Brownlee D. E. (1973) The development of microcrater populations on lunar rocks. *Proc. Lunar Sci. Conf. 4th*, p. 3213–3234.

Hartung J. B., Hörz F., and Gault D. (1972) Lunar microcraters and interplanetary dust. *Proc. Lunar Sci. Conf. 3rd*, pp. 2735–2753.

Hartung J. B. and Storzer D. (1974) Lunar microcraters and their solar flare track record. *Proc. Lunar Sci. Conf. 5th*, p. 2527–2541.

Hoffmann H. J., Fechtig H., Grün E., and Kissel J. (1975) First results of the micrometeoroid experiment S-215 on the HEOS 2 satellite. *Planet. Space Sci.* **23**, 215–224.

Hörz F., Brownlee D. E., Fechtig H., Hartung J. B., Morrison D. A., Neukum G., Schneider E., Vedder J. F., and Gault D. E. (1975) Lunar microcraters: Implications for the micrometeoroid complex. *Planet. Space Sci.* **23**, 151–172.

Hutcheon I. (1976) Reply to comments by Zinner and Morrison. *J. Geophy. Res.* **31**, 6367–6368.

Hutcheon I. D., Macdougall D., and Price P. B. (1974) Improved determination of the long term Fe spectrum from 1 to 460 NeV/amu. *Proc. Lunar Sci. Conf. 5th*, p. 2561–2576.

LSPET (1970) Preliminary examination of lunar samples . In *Apollo 12 Prelim. Sci. Rep.*, NASA SP-235, p. 189–215.

Mandeville J.-C. (1977) Microcraters on 12054 rock (abstract). In *Lunar Science VIII*, p. 613–615. The Lunar Science Institute, Houston.

McDonnell J. A. M. (1977) Accretionary particles: Production and equilibrium on 12054 (abstract). In *Lunar Science VIII*, p. 643–645. The Lunar Science Institute, Houston.

McDonnell J. A. M., Berg O. E., and Richardson F. F. (1975) Spatial and time variations of the interplanetary microparticle flux analyzed from deep space probes Pioneers 8 and 9. *Planet. Space Sci.* **23**, 205–214.

Morrison D. A., McKay D. S., Fruland R. M., and Moore H. V. (1973) Microcraters on Apollo 15 and 16 rocks. *Proc. Lunar Sci. Conf. 4th*, p. 3235–3253.

Morrison D. A. and Zinner E. (1975) Studies of solar flares and impact craters in partially protected crystals. *Proc. Lunar Sci. Conf. 6th*, p. 3373–3390.

Morrison D. A. and Zinner E. (1976a) Distribution and flux of micrometeoroids. In *The Moon—A New Appraisal from Space Missions and Laboratory Analyses*, p. 379–384. The Royal Society, London.

Morrison D. A. and Zinner E. (1976b) The size frequency distribution and rate of production of microcraters. In *Interplanetary Dust and Zodiacal Light* (H. Elsaesser and H. Fechtig, eds.), p. 227–231. Springer-Verlag, New York.

Nagel K., Fechtig H., Schneider E., and Neukum G. (1976) Micrometeorite impact craters on Skylab experiment S-149, In *Interplanetary Dust and Zodiacal Light* (H. Elsaesser and H. Fechtig, eds.), p. 275–278. Springer-Verlag, New York.

Nishiizuma K., Imamura M., Houda M., Russ G. P., III, Kohl C. P., and Arnold J. R., (1976) ^{53}Mn in the Apollo 15 and 16 drill stems: Evidence for surface mixing. *Proc. Lunar Sci. Conf. 7th*, p. 41–54.

O'Kelley G. D., Eldridge J. S., Schonfeld E., and Bell P. R. (1971) Abundances of primordial radionuclides K, Th and U in Apollo 12 lunar samples by nondestructive gamma spectrometry: Implications for origin of lunar soil. *Proc. Lunar Sci. Conf. 2nd*, p. 1154–1168.

Price P. B., Hutcheon I. D., Cowsik R., and Barber D. J. (1971) Enhanced emission of Fe nuclei in solar flares. *Phys. Rev. Lett.* **26**, 916–919.

Reedy R. C. (1977) Solar proton fluxes (abstract). In *Lunar Science VIII*, p. 795–797. The Lunar Science Institute, Houston.

Rhodes J. M., Blanchard D. P., Brannon J. C., Rodgers K. V., and Dungan M. A. (1977) Chemistry, classification and petrogenesis of Apollo 12 mare basalts (abstract). In *Lunar Science VIII*, p. 804–806. The Lunar Science Institute, Houston.

Schneider E., Storzer D., Mehl B., Hartung J. B., Fechtig H., and Gentner W. (1973) Microcraters on Apollo 15 and 16 samples and corresponding dust fluxes. *Proc. Lunar Sci. Conf. 4th*, p. 3277–3290.

Schonfeld E. (1970) Preliminary examination of the lunar samples from Apollo 12. *Science* **167**, 1325–1339.

Storzer D., Poupeau G., and Krätschmer W. (1973) Track exposure and formation ages of some lunar samples. *Proc. Lunar Sci. Conf. 4th*, p. 2363–2377.

Walker R. and Yuhas D. (1973) Cosmic ray production rates in lunar materials. *Proc. Lunar Sci. Conf. 4th*, p. 2379–2389.

Yuhas D. E. (1974) The particle track record in lunar silicates: Long-term behavior of solar and galactic VH nuclei and lunar surface dynamics. Ph.D. thesis, Washington University, St. Louis.

Yuhas D. E., Walker R. M., Reeves H., Poupeau G., Pellas P., Lorin J. C., Chetrit G. C., Berdot J. L., Price P. B., Hutcheon I., Hart H. R., Fleischer R. L., Comstock G. M., Lal D., Goswami J. N.,

and Bhandari N. (1972) Track consortium report on rock 14310. *Proc. Lunar Sci. Conf. 3rd*, p. 2941–2947.

Zinner E. and Morrison D. (1976) Comment on micrometeorites and solar flare particles in and out of the ecliptic by I. D. Hutcheon. *J. Geophys. Res.* **81**, 6364–6366.

Zinner E., Walker R. M., Chaumont J., and Dran J. C. (1977) Surface enhanced elements and microcraters in lunar rock 76215 (abstract). In *Lunar Science VIII*, p. 1044–1046. The Lunar Science Institute, Houston.

Zook H. A. and Berg O. E. (1974) A source for hyperbolic cosmic dust particles. *Planet. Space Sci.* **23**, 183–203.

Zook H., Hartung J., and Storzer D. (1976) Solar flare activity record as derived from lunar microcrater data (abstract). In *Lunar Science VII*, p. 968–970. The Lunar Science Institute, Houston.

Zook H., Hartung J., and Storzer D. (1977) Solar flare activity: Evidence for large scale changes in the past. *Icarus* In Press.